CHEMISTRY
A EUROPEAN JOURNAL

DOI: 10.1002/chem.200902568

Coexistence of Two Thermally Induced Intramolecular Electron Transfer Processes in a Series of Metal Complexes [M(Cat-N-BQ)(Cat-N-SQ)]/[M(Cat-N-BQ)$_2$] (M = Co, Fe, and Ni) bearing Non-Innocent Catechol-Based Ligands: A Combined Experimental and Theoretical Study**

Emi Evangelio,[a] Marie-Laure Bonnet,[b] Miquel Cabañas,[c] Motohiro Nakano,[d] Jean-Pascal Sutter,[e] Andrea Dei,[f] Vincent Robert,[b] and Daniel Ruiz-Molina*[a]

Abstract: The different thermally induced intermolecular electron transfer (IET) processes that can take place in the series of complexes [M(Cat-N-BQ)(Cat-N-SQ)]/[M(Cat-N-BQ)$_2$], for which M = Co (**2**), Fe (**3**) and Ni(**4**), and Cat-N-BQ and Cat-N-SQ denote the mononegative (Cat-N-BQ$^-$) or dinegative (Cat-N-SQ^{2-}) radical forms of the tridentate Schiff-base ligand 3,5-di-*tert*-butyl-1,2-quinone-1-(2-hydroxy-3,5-di-*tert*-butylphenyl)imine, have been studied by variable-temperature UV/Vis and NMR spectroscopies. Depending on the metal ion, rather different behaviors are observed. Complex **2** has been found to be one of the few examples so far reported to exhibit the coexistence of two thermally induced electron transfer processes, ligand-to-metal (IET^{LM}) and ligand-to-ligand (IET^{LL}). IET^{LL} was only found to take place in complex **3**, and no IET was observed for complex **4**. Such experimental studies have been combined with ab initio wavefunction-based CASSCF/CASPT2 calculations. Such a strategy allows one to solicit selectively the speculated orbitals and to access the ground states and excited-spin states, as well as charge-transfer states giving additional information on the different IET processes.

Keywords: electron transfer · magnetic properties · mixed-valent compounds · radicals · valence tautomerism

Introduction

Development of molecular-scale systems that exhibit intramolecular electron transfer (IET) phenomena induced by external stimuli has attracted considerable attention.[1] The interest is twofold. First, from a fundamental point of view, these complexes represent an excellent scenario to study the role of various parameters governing IET in molecular sys-

[a] Dr. E. Evangelio, Dr. D. Ruiz-Molina
Centro de Investigación en Nanociencia y Nanotecnología
(CIN2, CSIC-ICN), Edifici CM7, Campus UAB 08193
Cerdanyola del Vallès, Catalonia (Spain)
Fax: (+34) 93-5813717
E-mail: druiz@cin2.es

[b] Dr. M.-L. Bonnet, Dr. V. Robert
Laboratoire de Chimie, UMR 5182
École normale supérieure de Lyon
69364 Lyon cedex 07 (France)

[c] Dr. M. Cabañas
Servei de Ressonància Magnètica Nuclear, UAB
Campus de la UAB 08193
Cerdanyola del Vallès, Catalonia (Spain)

[d] Dr. M. Nakano
Department of Applied Chemistry
Graduate School of Engineering
Osaka University, Yamada-oka
Suita, Osaka 565-0871 (Japan)

[e] Dr. J.-P. Sutter
Laboratoire de Chimie de Coordination du CNRS (CNRS:LCC)
205, route de Narbonne, 31077 Toulouse (France)
and Université de Toulouse, UPS, INP, LCC

[f] Prof. A. Dei
Laboratory of Molecular Magnetism
Dept. of Chemistry, Polo Scientifico
Via della Lastrucia (Italy)

[**] Cat-N-BQ and Cat-N-SQ denote the mononegative (Cat-N-BQ$^-$) or dinegative (Cat-N-SQ^{2-}) radical forms of the tridentate Schiff-base ligand 3,5-di-*tert*-butyl-1,2-quinone-1-(2-hydroxy-3,5-di-*tert*-butylphenyl)imine.

Supporting information for this article is available on the WWW under http://dx.doi.org/10.1002/chem.200902568.

tems. And second, the possibility to induce a reversible change in the electronic distribution of a molecular system has opened the door to their potential use as information storage and integrated molecular-sized devices. Mixed-valence systems are exceptional candidates for such studies since they contain at least two redox sites with different oxidation states linked by a bridge that mediates the electron transfer from one site to the other.[2] The study of molecular mixed-valence systems was initiated by Taube's seminal work on ruthenium compounds, such as $[(NH_3)_5Ru\text{-bridge-}Ru(NH_3)_5]^{5+}$.[3] Since then, most of the reported mixed-valence complexes, which exhibit IET phenomenon, are homo- and heterometallic complexes[4] or metallocene[5] units in which the two metal atoms with different oxidation states are connected through an organic bridging ligand.

In contrast, mixed-valence molecular systems in which the electroactive units are purely organic have received less attention so far, probably owing to their high instability.[6] Nevertheless, the flexibility of organic synthesis may afford the preparation of purely organic, mixed-valence molecular wires with the specific and sophisticated topologies required in the demanding and ever-increasing world of nanotechnology. Moreover, the study of their properties should lead to the synthesis of systems in which the electron transfer could be finely tuned in a far more precise way than have been done with coordination compounds. Representative examples of the different types of electroactive organic units so far used are: i) anion radicals derived from conjugated diquinones and diimides,[7] ii) cation radicals derived from bis(tetrathiafulvalenes),[8] iii) cation radicals derived from bis(hydrazines),[9] iv) quinoid groups,[10] and v) ion radicals derived from π-conjugated polyarylmethyl/polyarylamines/polychlorotriphenylmethyl radicals[11] and bridged dinitroaromatic radical and bis(dioxaborine)anions mixed-valence systems[12] among others.

Most of the examples previously described are based on pure organic systems in which both electroactive units are linked through an organic bridge, whereas the number of systems with the electroactive units linked through a metal ion are less frequent.[13] Under such a scenario, redox-active organic ligands are electronically coupled to an extent that is regulated by the orbital interactions with the metal ion bridge.[14] One such rare example is the family of ruthenium and rhenium polynuclear complexes bearing redox-active bipyridinium ligands reported by Abe et al.[15] These authors showed that metal-cluster units often behave as redox mediators in spite of their large size and of the remote distance of the ligand-based redox centers.

Very recently, we also reported a new family of systems where the thermally induced IET between organic electroactive units takes place through a metal ion. Such a family consists of transition-metal complexes containing at least two redox-active catecholate or phenoxylate ligands with different oxidation states. For instance, IET between catechol units in the complex [Co(3,5-DTBCat)(3,5-DTBSQ)(bpy)] (**1**) in which 3,5-$DTBCat^{2-}$ and 3,5-$DTBSQ^{-}$ refer to the catecholate (Cat^{2-}) and semiquinonate (SQ^{-}) forms of 3,5-di-*tert*-butyl-*o*-quinone, respectively, was shown to take place.[16] Even more interesting was the fact that this complex also exhibits a reversible thermally induced IET between the metal ion and the ligand, a process named with the generic term of valence tautomerism (VT).[17] Therefore, this family of complexes contains unique systems that exhibit more than one type of thermally induced, intramolecular, electron-transfer process—ligand-to-metal (IET^{LM})[18] and ligand-to-ligand (IET^{LL}).[19] A schematic representation of the different thermally induced IET processes that take place in a metal-based complex bearing catechol-based non-innocent ligands is shown in Figure 1.

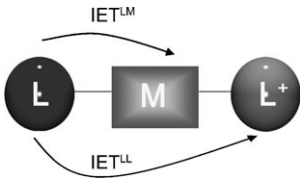

Figure 1. Graphical representation of the different thermally induced IET processes that may take place in a complex schematized with a metal ion (square) and two catechol-based non-innocent ligands (spheres) with different oxidation state.

To what extent IET^{LM} and IET^{LL} can coexist within this family of complexes remains an open issue of considerable interest. For this reason we have focused our attention in the study of catechol-bearing complexes involving multiple electron-transfer phenomena. With this aim, an excellent model to study is the series of complexes [M(Cat-N-BQ)(Cat-N-SQ)]/[M(Cat-N-$BQ)_2$] in which M = Co (**2**),[20] Fe (**3**), and Ni (**4**).[21] The tridentate Schiff-base ligand 3,5-di-*tert*-butyl-1,2-quinone-1-(2-hydroxy-3,5-di-*tert*-butylphenyl)-imine[22] leads to stable coordination complexes with several metal ions, and exhibit different oxidation states ranging from 0 to −3 (see Scheme 1). Nevertheless, it usually coordinates in the mononegative Cat-N-BQ^{-} or dinegative Cat-N-SQ^{2-} radical forms[23] generating mixed-valence species. Although complexes **2**–**4** have been previously synthesized, only preliminary studies on the IET^{LM} of complex **2** have been reported.[24] In this work their variable-temperature behavior has been studied in detailed by complementary spectroscopic techniques, mainly UV/Vis and NMR, and solution magnetic measurements. Such experimental studies have been combined with ab initio complete active space self-consistent field (CASSCF) calculations and subsequent second-order perturbation theory treatment (CASPT2) to clarify the underlying electron distributions in the ground and speculated excited states. Depending on the metal ion, rather different IET processes are evidenced and theoretically rationalized. Particular attention has been paid to the versatility of the electroactive ligand as the metal center is changed.

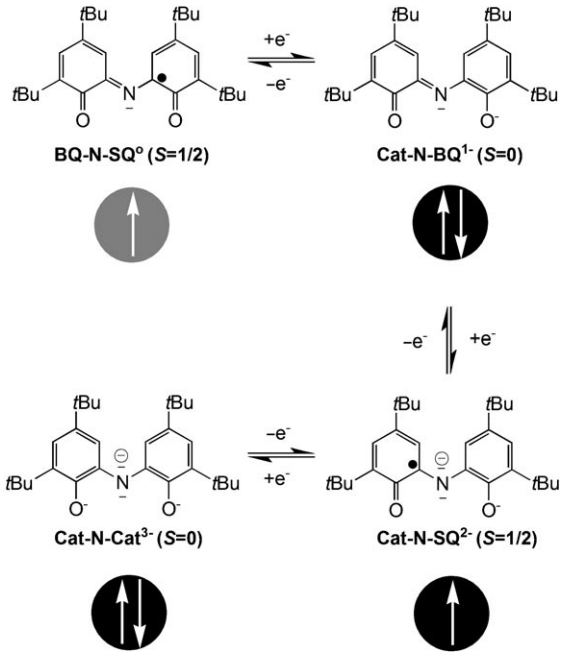

Scheme 1. Different oxidation states that can be found for the Schiff-base iminoquinone ligand in a transition metal complex.

Results

UV/Vis spectroscopy: In previous work, Girgis et al[22c] predicted that most of the bands observed in the electronic spectra of complexes with the general formula ML_2 (L = Cat-N-BQ^-/Cat-N-SQ^{2-}) are associated with electronic transitions within the ligand. Previous density functional studies on related catechol-based systems to assign electronic transitions have already been published.[18]

Among them, the band centered at $\lambda = 390$ nm is of especial interest. This band can be attributed to the radical character of the Cat-N-SQ^{2-} ligand giving direct information on its oxidation state and therefore on the electronic distribution of the complex at a given temperature. To support this assignment, the UV/Vis spectra of model complexes [Ga(Cat-N-SQ)(Cat-N-BQ)] (**5**) and [Zn(Cat-N-$BQ)_2$] (**6**) were recorded and studied for comparison purposes. As expected, complex **6** shows two intense bands at $\lambda = 793$ and 736 nm tailing into the near-IR region lacking any band in the $\lambda =$ 350–400 nm region, since both ligands display the non-radical form Cat-N-BQ^-. In contrast, the electronic spectrum of complex **5** is dominated by an intense transition at $\lambda =$ 390 nm associated with the presence of the Cat-N-SQ^{2-} radical ligand.

Variable-temperature UV/Vis experiments on a solution of complex **2** in toluene were analyzed in the 200–360 K temperature range. The choice of toluene is justified both on the basis of the high solubility of complex **2** and its broad working temperature range. Under these conditions, IET^{LM} can be induced by temperature variations and monitored by UV/Vis spectroscopy (see Figure 2b). In the low-temperature regime, a spectrum reminiscent of that of complex **5** was obtained, with bands at $\lambda = 439$ and 533 nm and especially at $\lambda = 391$ nm, associated with the presence of the Cat-N-SQ^{2-} radical ligand (no bands in the near-IR region that could be attributed to an intervalence band transition were observed). Therefore, the **2**,*ls*-Co^{III} ($S = 1/2$) tautomer is found to be the predominant form at low temperatures. As the temperature is increased, the ligand-to-metal electron transfer is activated, as one of the ligands evolves from a Cat-N-SQ^{2-} radical to a Cat-N-BQ^- diamagnetic ligand [Eq. (1)]:

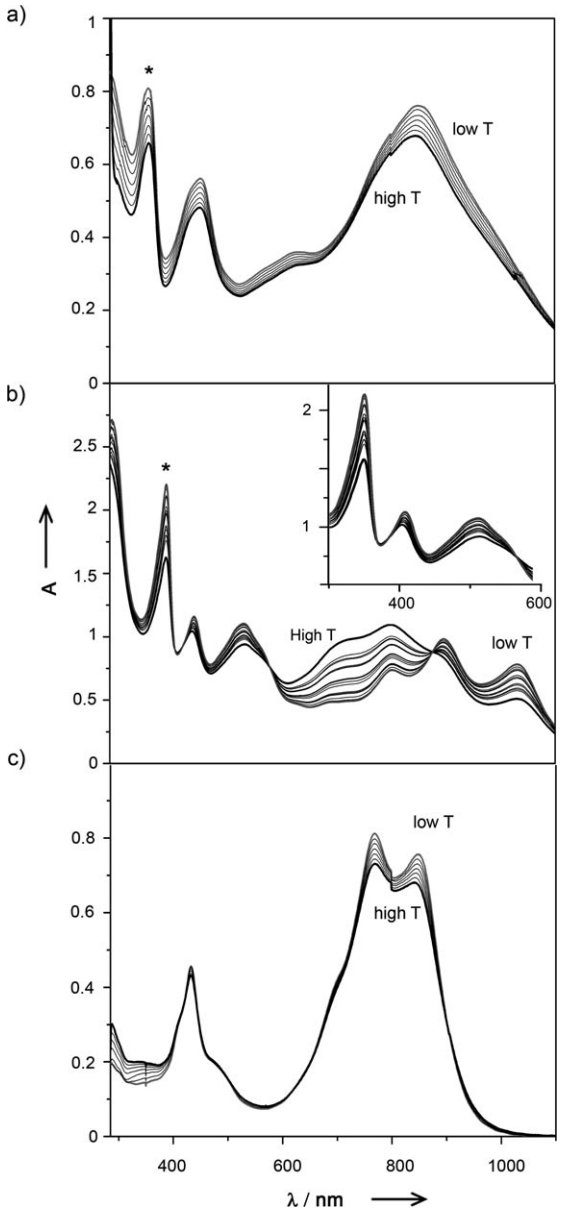

Figure 2. Variable-temperature UV/Vis spectra (203–363 K) for complexes: a) [Fe(Cat-N-SQ)(Cat-N-BQ)] (**3**), b) [Co(cat-N-SQ)(Cat-N-BQ)] (**2**), and c) [Ni(Cat-N-BQ_2] (**4**). The band associated to the radical character of the ligand is marked with an asterisk.

$$[Co^{III}(Cat\text{-}N\text{-}BQ)(Cat\text{-}N\text{-}SQ)] \rightleftharpoons [Co^{II}(Cat\text{-}N\text{-}BQ)_2] \quad (1)$$

Thus, the **2**,*ls*-Co^{III} ($S=1/2$) tautomer converts into **2**,*hs*-Co^{II} ($S=3/2$). As a consequence the intensity of the band at $\lambda=391$ nm decreases, as well as those at $\lambda=439$ and 533 nm, whereas the bands at $\lambda=721$ and 797 nm, characteristic of the **2**,*hs*-Co^{II} tautomer, increase in intensity (see Figure 2b). Two isobestic points appear at $\lambda=856$ and 590 nm, confirming that at least two species are interconverting under the studied temperature range.

Variable-temperature UV/Vis experiments on a toluene solution of the analogous iron complex **3** were also studied (Figure 2a). Bands at $\lambda=357$, 451 and 853 nm with shoulders around $\lambda=560$, 620, and 790 nm can be observed in the low-temperature regime. The observation of the band at $\lambda=357$ nm is an indication that the iron complex **3** has one ligand in its radical form, Cat-N-SQ^{2-}, remaining, therefore, in the [Fe(Cat-N-SQ)(Cat-N-BQ)] (**3**,*ls*-Fe^{III}) form. However, by contrast with the cobalt complex **2**, only a slight variation of the bands intensity, without the presence of any isobestic point, was detected after an increase in the temperature. Such spectral variations may be associated with variations of the solution viscosity, among others, rather than the existence of IET^{LM}. Therefore, complex **3** remains in its **3**,*ls*-Fe^{III} tautomeric form over the whole temperature range studied. In contrast, the UV/Vis spectrum of the nickel complex **4** (see Figure 2c) exhibits bands at $\lambda=432$, 766 and 846 nm with a shoulder around $\lambda=690$ nm, reminiscent of that observed for complex **6**. Moreover, temperature variations do not induce any considerable change in the electronic spectrum, only a slight variation of the band intensity is observed. The presence and intensity of the two bands at higher wavenumbers, as well as the lack of the characteristic radical band, support the presence of the **4**,*hs*-Ni^{II} tautomeric form over the whole temperature range studied. These results were confirmed by magnetization measurements.

Magnetization measurements

Solution measurements: The magnetic behavior of complexes **2**–**4** in solution was studied by NMR spectroscopy by using the Evans method.[25] This technique is used to measure the magnetic susceptibility of paramagnetic species based on the frequency shift that it originates in the NMR signal of a standard diamagnetic compound, for instance TMS. The μ_{eff} versus T plot for a solution of complexes **2**–**4** in toluene obtained by applying the Evans method is shown in Figure 3. At low temperatures, the μ_{eff} versus T plot of complex **2** exhibits a value of 1.84 μ_B close to the theoretical value of 1.73 μ_B expected for the single unpaired electron of the **2**,*ls*-Co^{III} ($S=1/2$) tautomer. An increase of the temperature induces a gradual increase of μ_{eff} till a maximum value of 4.53 μ_B is reached at 353 K, close to the theoretical value for a $S=3/2$ species with a large unquenched orbital contribution. This experimental fact corroborates the existence of an equilibrium between the **2**,*ls*-Co^{III} ($S=1/2$) and **2**,*hs*-Co^{II} ($S=3/2$) tautomers, as previously observed by UV/Vis data.

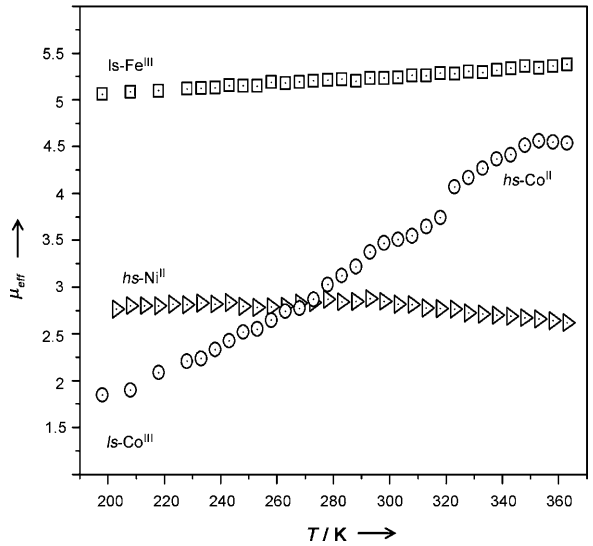

Figure 3. Representation of μ_{eff} versus T obtained by the Evans Method in the 203–363 K temperature range for complexes **2** (○), **3** (□) and **4** (△).

Under these conditions, one may track the thermodynamic parameters associated with the rearrangement of the electronic configuration in writing $\chi_m T$ as Equation (2) with Equation (3):

$$\chi_m T = \chi_m T_{ls\text{-}Co^{III}} + \gamma_{hs\text{-}Co^{II}}\,(\chi_m T_{hs\text{-}Co^{II}} - \chi_m T_{ls\text{-}Co^{III}}) \quad (2)$$

$$\gamma_{hs\text{-}Co^{II}} = 1/[\exp(\Delta H/RT - \Delta S/R) + 1] \quad (3)$$

in which $\chi_m T_{ls-Co^{III}}$ and $\chi_m T_{ls-Co^{II}}$ are the $\chi_m T$ values for isolated **2**,*ls*-Co^{III} ($S=1/2$) and **2**,*hs*-Co^{II} ($S=3/2$), respectively, and $\gamma_{hs-Co^{II}}$ is the molar fraction of **2**,*hs*-Co^{II}. If $\chi_m T_{ls-Co^{III}}$ and $\chi_m T_{hs-Co^{II}}$ are fixed to the values of 1.84 and 4.53 μ_B, the least-square fitting of $\chi_m T$ to Equation (3) gives values of $\Delta H=28.2$ kJ mol^{-1} and $\Delta S=95.2$ J K^{-1} mol^{-1} ($T_c=\Delta H/\Delta S=296$ K).

The μ_{eff} versus T plots of complexes **3** and **4** are also shown in Figure 3 for comparison purposes. Complex **3** exhibits a constant magnetic susceptibility value over the whole temperature range of approximately 5.20 μ_B. This value can be explained if we consider that the main species in solution along the whole temperature range is the [Fe(Cat-N-BQ)(Cat-N-SQ)] (**3**,*ls*-Fe^{III}) tautomer. These results are in agreement with our electronic spectra analysis previously described, which show the characteristic band of the radical Cat-N-SQ^{2-} ligand around $\lambda=350$ nm. In this species, a strong antiferromagnetic interaction between the radical ligand Cat-N-SQ^{2-} ($S=1/2$) and the *hs*-Fe^{III} ion ($S=5/2$) leads to a $S=2$ magnetic ground state for which a theoretical value of 4.90 μ_B is expected (the expected μ_{eff} value for a non-interacting *hs*-Fe^{III} and a organic radical would be 6.16 μ_B). Similar behavior was observed for complex **4**, which exhibits a constant magnetic susceptibility value of approximately 2.83 μ_B over the whole temperature range.

This is the expected value for a $S=1$ magnetic state attributed to the *hs*-Ni^{II}.

Solid-state measurements: The magnetic properties of complex **2** have already been described in a previous work by Dei et al.[20b] These authors showed that complex **2** exhibits a tautomeric interconversion in the solid state, but at much higher temperatures than in solution, with a transition that starts at approximately 370–380 K, at least 150 K higher than in solution. Thus, in this work only the temperature-dependent magnetic susceptibility for crystalline samples of complexes **3** and **4** (which has not been previously described) over the 5–400 K temperature range with an applied external field of 10 kG was measured. At high temperatures, complexes **3** and **4** are characterized by μ_{eff} values of 4.7 and 3.1 μ_B, respectively. This value remains constant down to approximately 30 K, whereupon it gradually decreases most likely owing to the presence of small intermolecular antiferromagnetic exchange interactions and/or the zero-field-splitting effect for these ions. For complex **4**, such a value is close to the theoretical value of 2.83 μ_B expected for the **4**,*hs*-Ni^{II} ($S=1$) tautomer with both ligands in the diamagnetic form Cat-N-BQ^-; confirming that complex **4** also remains *hs*-Ni^{II} even down to very-low temperatures in the solid state. The μ_{eff} value of complex **3** can be explained if we consider that the main species in the solid state over the whole temperature range is [Fe(Cat-N-BQ)(Cat-N-SQ)] (**3**,*ls*-Fe^{III}). Such isomer bears a radical Cat-N-SQ^{2-} ligand antiferromagnetically coupled with the iron ion, in agreement with the solution measurements previously described.

^{1}H NMR experiments: The ^{1}H NMR spectra of complexes **2**–**4** were recorded and the signal of the *tert*-butyl (*t*Bu) groups monitored over the whole temperature range. The data from variable-temperature ^{1}H NMR experiments of a solution of complex **2** in toluene in the 203–363 K temperature range is shown in Figure 4. The high-temperature spectrum, in which the dominant species is the **2**,*hs*-Co^{II} tautomer, exhibits two main signals, each one embracing four *t*Bu groups. This detail is in agreement with the theoretical expectations. Indeed, as the **2**,*hs*-Co^{II} tautomer bears two symmetrical monoanionic Cat-N-BQ^- ligands, the eight *t*Bu groups of the complex are expected to be equivalent 4:4 depending on whether they are located at the *para* or *ortho* positions of the oxygen atom. Therefore, only two main broad signals should be observed. A temperature decrease induces an interconversion from the **2**,*hs*-Co^{II} to the **2**,*ls*-Co^{III} tautomer, which is followed by a remarkable shift of the *t*Bu signals with chemical shifts as large as $\Delta\delta=-7.2$ and $\Delta\delta=3.1$ ppm. Such remarkable variations arise from the electronic rearrangement experienced by the complex along the valence tautomeric interconversion. The spin density is localized on the metal ion in the **2**,*hs*-Co^{II} tautomer, whereas it shifts to the (Cat-N-$SQ)^{2-}$ ligand in the **2**,*ls*-Co^{III} form, resulting in a larger paramagnetic shift and broadening of the peaks. Even more remarkable is the fact that only two main peaks are still observed even at very-low temperatures. This observation is rather unexpected, as the **2**,*ls*-Co^{III} tautomer bears two ligands with different oxidation states, Cat-N-BQ^- and Cat-N-SQ^{2-}. Accordingly, the *t*Bu groups should no longer be equivalent 4:4, but instead 2:2, and at least four different peaks should be observed at low temperatures. This unexpected observation is likely the signature of an electron delocalization of the extra electron over both ligands, that is, an IET^{LL} takes place on the time scale of the experiment.

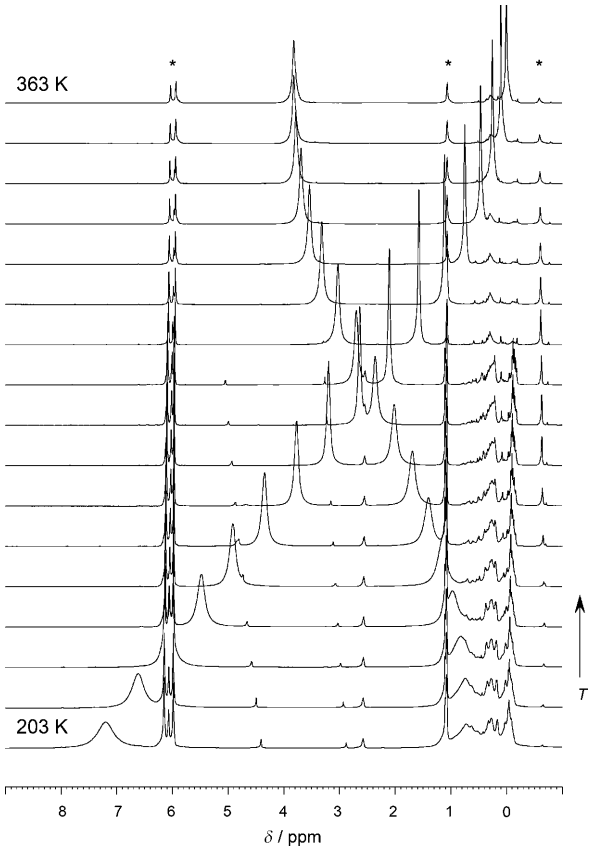

Figure 4. ^{1}H NMR (400 MHz) shift peak of the *t*Bu groups in the iminoquinone ligand for complex **2** as a function of temperature (203 K to 363 K) in [D_8]toluene. Each intermediate spectrum corresponds to increments of 10 K of temperature. Solvent peaks are marked with an asterisk.

Variable-temperature ^{1}H NMR experiments of solutions of complexes **3** and **4** in toluene in the 203–363 K temperature range were also studied (related values are given in the Supporting Information). As previously described for complex **2**, only two types of peaks associated with the *t*Bu groups are observed in both cases over the whole temperature range. The observation of only two signals is in agreement with the expectations for complex **4**. This complex remains in its **4**,*hs*-Ni^{II} tautomeric form bearing two symmetrical monoanionic Cat-N-BQ^- ligands and, therefore, with the *t*Bu groups equivalent 4:4. Nevertheless, such an argument is not valid for complex **3**, which stays mostly in its **3**,*ls*-Fe^{III} form and therefore four instead of two *t*Bu peaks should be observed. This has been explained previously for **2**,*ls*-Co^{III},

with the presence of a fast IET converting both ligands with different oxidation states Cat-N-BQ^{-} and Cat-N-SQ^{2-} to be non-distinguishable. Such remarkable differential shifts are also experienced by the *t*Bu signals of complexes **2**–**4**. Such differential behavior is better illustrated in Figure 5, in which the same behavior for complex **6** has also been included for comparison purposes. The chemical shifts of the two *t*Bu groups signals for complex **2** vary considerably ($\Delta\delta = -3$ and 7 ppm). Interestingly, a crossing occurs at approximately 285 K, a temperature that is close to the $T_c =$ 296 K value extracted from the solution-magnetization data. In this region, the VT tautomerism makes the *t*Bu groups shifts equivalent ($\approx$5.8 ppm), as both IET^{LM} and IET^{LL} electron transfers average the local-spin densities. In contrast, the chemical-shift changes are smaller for complex **3** ($\Delta\delta =$ -3 and 5 ppm) and almost negligible for complex **4** ($\Delta\delta =$ -0.5 and 1 ppm) (detailed values are given in Tables S1–S3 in the Supporting Information). As expected, the paramagnetic shift of the *t*Bu groups for complex **3** is larger than for complex **4**, as the presence of the unpaired electron in the same ligand through its Cat-N-SQ^{2-} form induces a larger paramagnetic shift. Moreover, there is no crossing between the chemical shifts of *t*Bu groups, a reflection of the lack of VT in complexes **3** and **4**.

Quantum-chemical calculations: To support the conclusions drawn from experimental data, ab initio wavefunction based calculations were performed on complexes **2**–**4**. The calculations were carried out by using the X-ray geometries without any additional structural optimization. To account for possible charge transfers (i.e. IET^{LM} and IET^{LL}) between the ligand and the metal ions, specific spin states were considered for the three systems. Such strategy allows one to solicit selectively the speculated orbitals and to access the ground states and excited-spin states, as well as charge-transfer states. The resulting CASPT2 energies for complexes **2**–**4**, referenced to the ground state (GS) energy, are summarized in Table 1. The energy difference (ΔE) corresponds to vertical transitions calculated by using the reported structures of each complex (so-called intervalence transition in mixed-valence compounds). Following the theory developed by Hush,[26] the intervalence band energy (ΔE) is

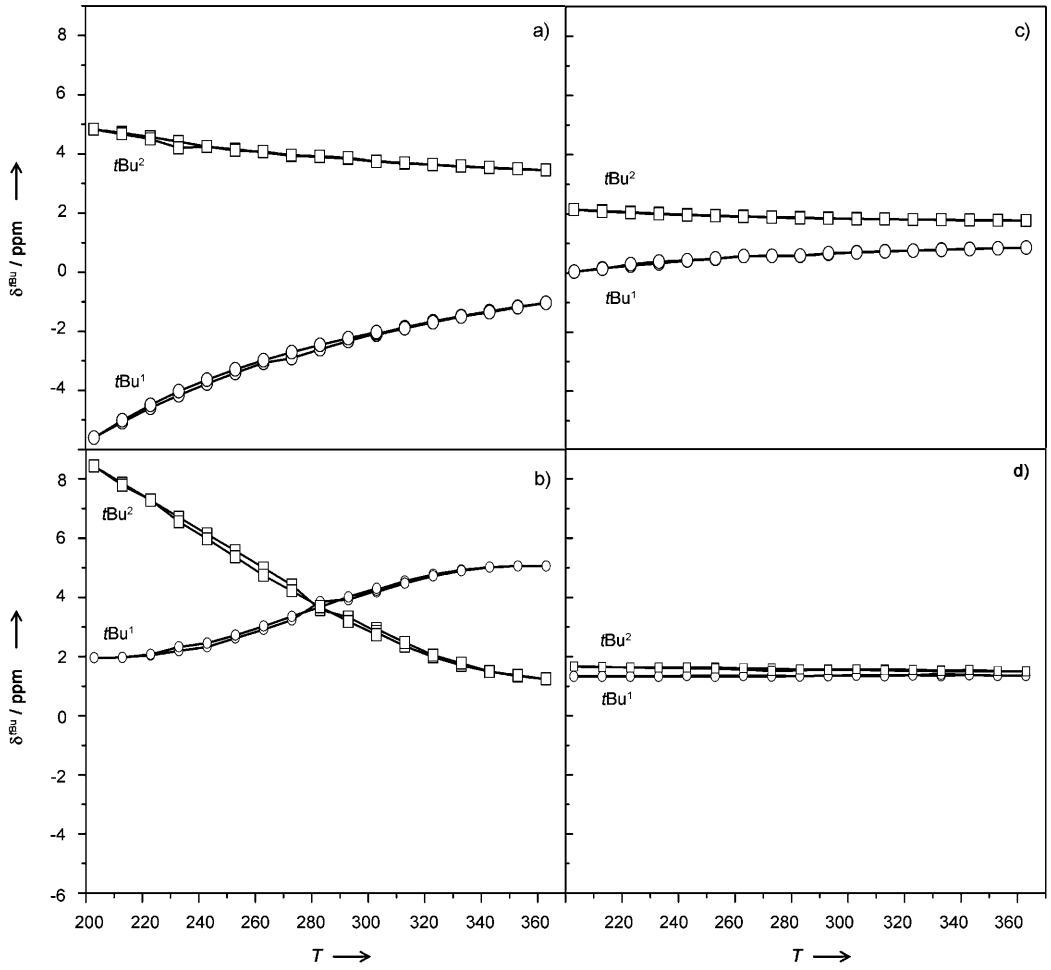

Figure 5. Representation of the *t*Bu shift peaks vs. temperature for a) complex **3**, b) complex **2**, c) complex **4**, and finally d) diamagnetic complex **6**, as a model compound.

Table 1. Ground and IET states nature. ΔE and δE stand for the vertical transitions energies (cm^{-1}) associated to LM and LL electron transfers.

Complex	GS / spin state	Tautomer / spin state	ΔE	δE
2	*ls*-Co^{III} / $S=1/2$	*hs*-Co^{II} / $S=3/2$	4500	700
3	*ls*-Fe^{III} / $S=2$	*hs*-Fe^{II} / $S=2$	13500	500
4	*hs*-Ni^{II} / $S=1$	*ls*-Ni^{III} / $S=1$	31000	500

the sum of the reorganization energy (λ) and the energy difference between the tautomers ($\Delta G°$) (see Figure 6 for notations).

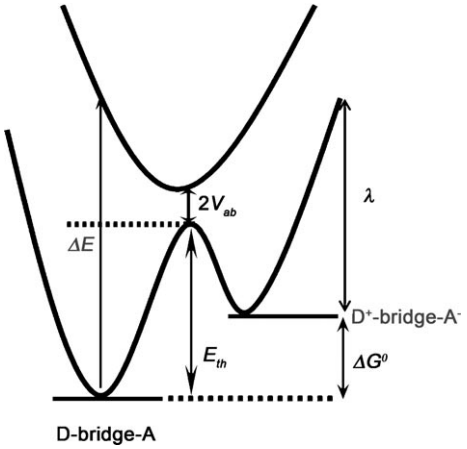

Figure 6. Non-adiabatic potential energy curves. ΔE and λ correspond to the vertical energy transition and reorganization energy, respectively.

As the reorganization energy (mainly electrostatic) is expected to be similar in all complexes, one can assume that the adiabatic energy difference is mainly controlled by the vertical transition energies ΔE (Figure 6). Thus, as ΔE increases, the intramolecular electron transfers should be reduced. A detailed inspection of the electron-transfer kinetic falls in the Hush's[26] theory, but is out of the scope of the present study.

In light of our experimental results, there is strong evidence for interligand electron delocalization (IET^{LL}). Thus, the energy differences δE (Table 1) arising from the two speculated electron localization scenario were calculated for the [M(Cat-N-BQ)(Cat-N-SQ)] forms, M = Co, Fe.

For the nickel complex **4**, the lowest triplet CAS[4,2]SCF solutions were converged; the active orbitals are shown in Figure 7. The ground state is consistent with a d^8 Ni^{II} ion, holding two unpaired electrons in the mainly $d_{x^2-y^2}$ and d_{z^2} atomic orbitals in a distorted octahedral environment. Since the complex geometry displays quasi-orthogonality of the ligands, the π-ligand orbitals are almost orthogonal. Thus, one may wonder how efficient is the ligand-to-ligand intramolecular electron transfer. The higher lying triplet states exhibit one d-type and a mainly π-ligand based MOs (see Figure 8). The relative proximity ($500\ cm^{-1}$) of these two states strongly suggests an effective IET^{LL}. These triplet states correspond to a ferromagnetic interaction between a ligand and an orthogonal d-type (either $d_{x^2-y^2}$ or d_{z^2}) orbital. This ground state electronic picture is consistent with a d^7 Ni^{III} ion, one electron being transferred from the Ni^{II} to the ligand Cat-N-BQ^-. At a CASPT2 level of calculation, the energy difference ΔE is $31\,000\ cm^{-1}$, thus ruling out the possibility of the coexistence of Ni^{II} and Ni^{III}. The first excited state is, as expected from Tanabe–Sugano diagram, a Ni^{II} singlet lying $16\,000\ cm^{-1}$ above the GS triplet.

A similar strategy was used for the iron complex **3** that may display either five or six electrons (i.e. Fe^{III} or Fe^{II}) mostly localized on the Fe ion. By allowing six electrons in seven MOs in a CAS[6,7]SCF calculation, the active space is flexible enough to allow the occupations of the five Fe d-orbitals and either one of the ligand orbitals. The two lowest septet ($S=3$) states solutions were first converged since this particular spin multiplicity forces the single occupation of the active MOs, one of them being a ligand orbital similar to the ones shown in Figure 7. Starting from this set of MOs, the lowest quintet ($S=2$) states energies were calculated.

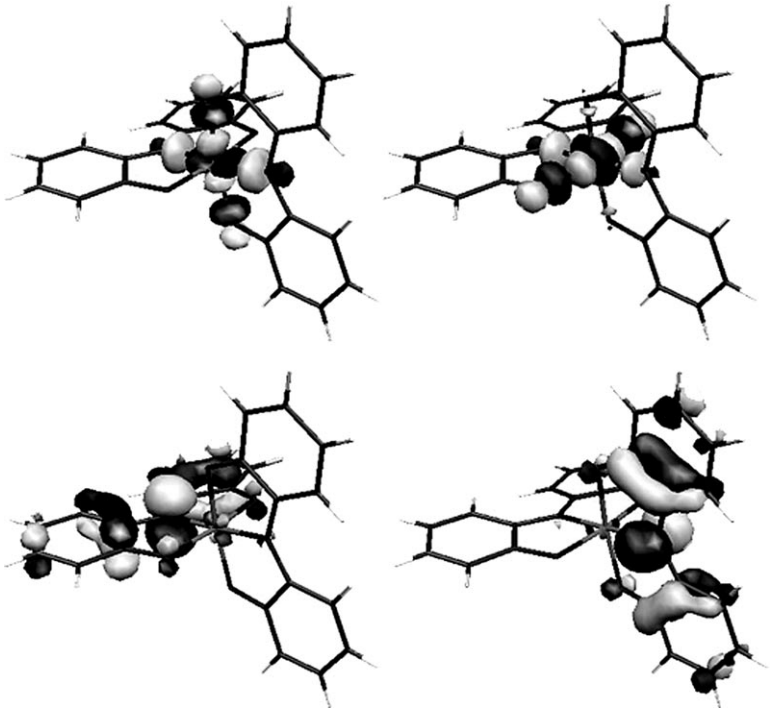

Figure 7. Active molecular orbitals (MOs) of complex **4**.

From the correlated wavefunction analysis, the ground spin state arises from the antiferromagnetic coupling between an *hs*-Fe^{III} ($S=5/2$) and a Cat-N-SQ^{2-} radical ($S=1/2$). Interestingly, another quintet lies relatively close in energy ($\Delta E=500\ cm^{-1}$) and corresponds to a similar picture, involving the second Cat-N-SQ^{2-} radical (Figure 8). The next quintet state displays six electrons in the d-type MOs of a high-spin Fe^{II} center. Clearly, such an electronic configuration accounts for the ligand-to-metal intramolecular electron transfer, while the energy difference ΔE is $13500\ cm^{-1}$ disposes of the participation of the Fe^{II}-Cat-N-BQ^{-} configuration. In agreement with our experimental data, **3** is likely to undergo IET^{LL} at room temperature, whereas VT is unlikely to occur.

The low-energy spectra for complex **2** exhibit three competing states that reflect the simultaneous presence of intramolecular and interligand charge transfers. The strategy we used to evaluate the energy levels ordering in **2**, is very similar. Starting from a CAS[7,7]SCF, the lowest lying quartet ($S=3/2$) and two doublets ($S=1/2$) were determined to identify the possible electron-hopping phenomena. As experimentally evidenced, the spectrum exhibits two close in energy-doublet states ($\Delta E=700\ cm^{-1}$) consisting formally of a d^7 Co^{III} ion and one unpaired electron in a mainly Cat-N-SQ^{2-} ligand π-orbital. Nevertheless, our ab initio calculations favor a quartet state (i.e. d^6 Co^{II}), as the Co complex ground state, whereas experimental data supports a doublet state. The lack of structural information as valence tautomerism occurs might be responsible for the ordering of the spin states. However, the vertical energy difference between the tautomers is much reduced, as compared to complexes **3** and **4**. From our ab initio calculations, the ability of one electron to get delocalized over three partners is shown to

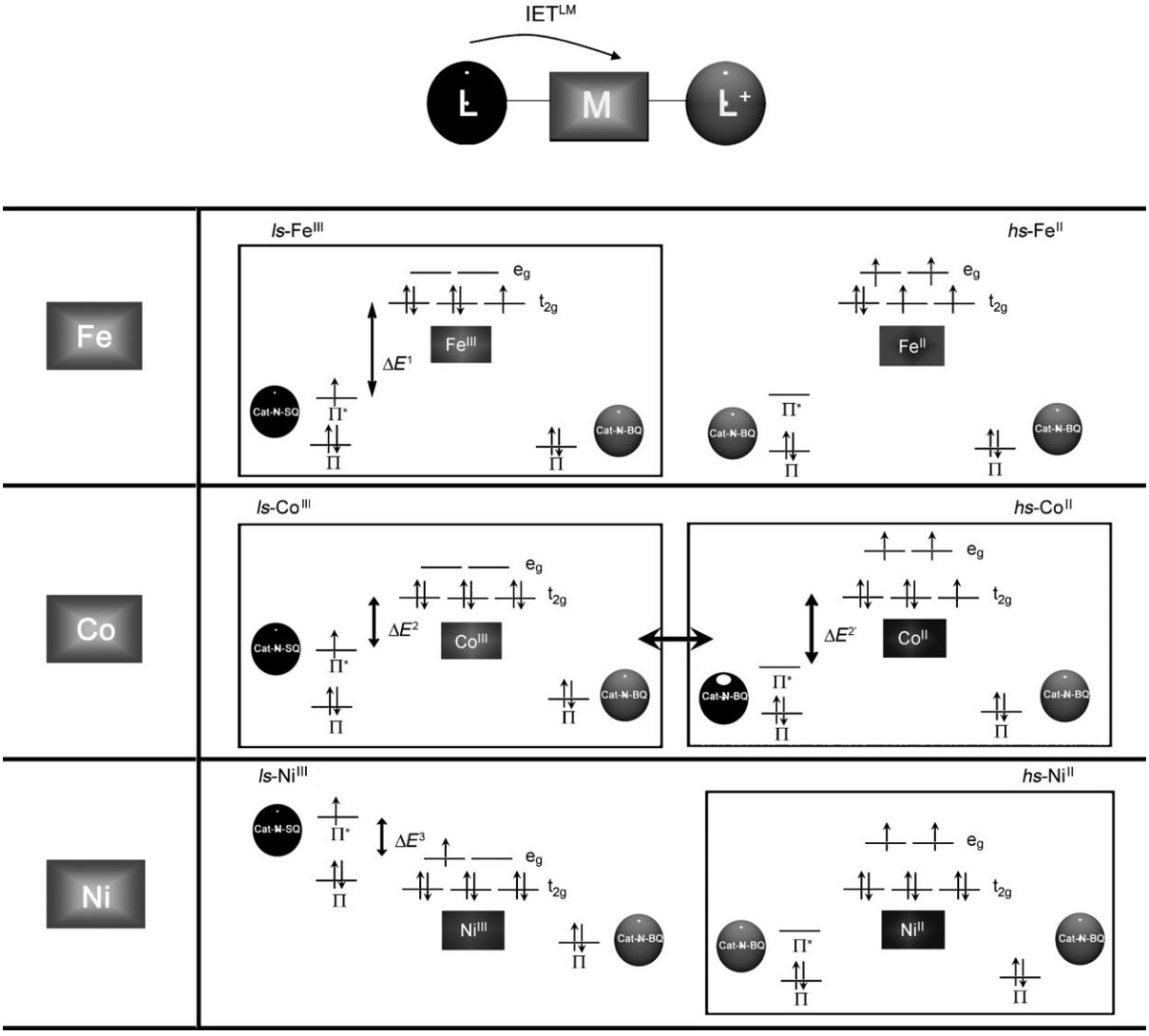

Figure 8. Schematic representation of the simplified MOs energies for complexes **2**–**4**. In the case of complex **3** the energy difference between the electroactive ligand and the iron ion is too large to allow for IET^{LM}. In the case of complex **2**, the energy difference with the cobalt ion orbitals is reduced and therefore resonating forms are observed along the temperature range studied (middle). And finally, the orbital energetics of the metal ion and the electroactive ligand in the case of complex **4** favors the population of the high-spin isomer over the whole temperature range.

generate a variety of spin states, which compete at room temperature, as evidenced by experimental data.

Discussion

Valence tautomerism or IET^{LM}: Experimental and theoretical results indicate that the **3**,*ls*-Fe^{III} tautomer remains much lower in energy than that of the **3**,*hs*-Fe^{II} tautomer over the whole temperature range studied, both in solution and solid state (Figure 9). Therefore, the intramolecular electron transfer between the imino ligand and the metal ion (IET^{LM}) in complex **3**, that is, valence tautomerism, does not take place. In other words, as far as the ligand-to-metal electron transfer is concerned, complex **3** can be considered most likely as a Class I or Class II with a very-large activation energy, according to the classification of Robin and Day.[27] Even if the molecule acquires sufficient activation energy to reach the intersection region, the probability of electron exchange would be null or very small in the studied temperature range, as a result of a rather weak interaction between the imino ligand and the iron ion. In contrast, the tautomeric form **4**,*hs*-Ni^{II} remains much lower in energy ($\approx$31 000 cm^{-1}) than the **4**,*ls*-Ni^{III} isomer, which is not detected within the temperature range measured. Thus, IET^{LM} is so effective that valence tautomerism is not observed in the nickel derivative **4** over the studied temperature range. Finally, the energy gap between the **2**,*ls*-Co^{III} and **2**,*hs*-Co^{II} tautomers gets smaller and interconversion can be thermally activated. Therefore, even though **2**,*ls*-Co^{III} is energetically more stable, a temperature increase induces IET from the ligand Cat-N-SQ^{2-} to the Co^{III} ion (i.e. the VT interconversion). Thus, complex **2** can be formally considered as a Class II system in which the interaction between the redox centers is moderate. In the vicinity of the conical intersection, a moderate energy lift arising from vibronic interactions tends to localize the electron in one of the redox centers. Nevertheless, the activation barrier can be overcome by an external stimulus giving rise to IET process. Such differential behavior is conceptually represented in Figure 8, through a comparative schematic representation of the highest occupied molecular orbitals (both HOMO and SOMOs) energies for each one of the tautomeric forms involved in the IET^{LM} process. The thermodynamically ground states for each complex are marked with a square. Only in the case of the cobalt complex are both tautomeric forms are thermodynamically accessible.

The differential VT behavior along the series of complexes **2**–**4** can be tentatively assigned to the different ionization potentials of the Co, Fe, and Ni metal ions and their overlap with the iminoquinone ligand π orbitals. Only in the case of the cobalt is there a good overlap between the relative energies of the metal ion and ligand-centered orbital. This situation can be reverted for another family of ligands, such as, VT in related Fe and Ni complexes that exhibit a good matching between the d and π orbitals has been al-

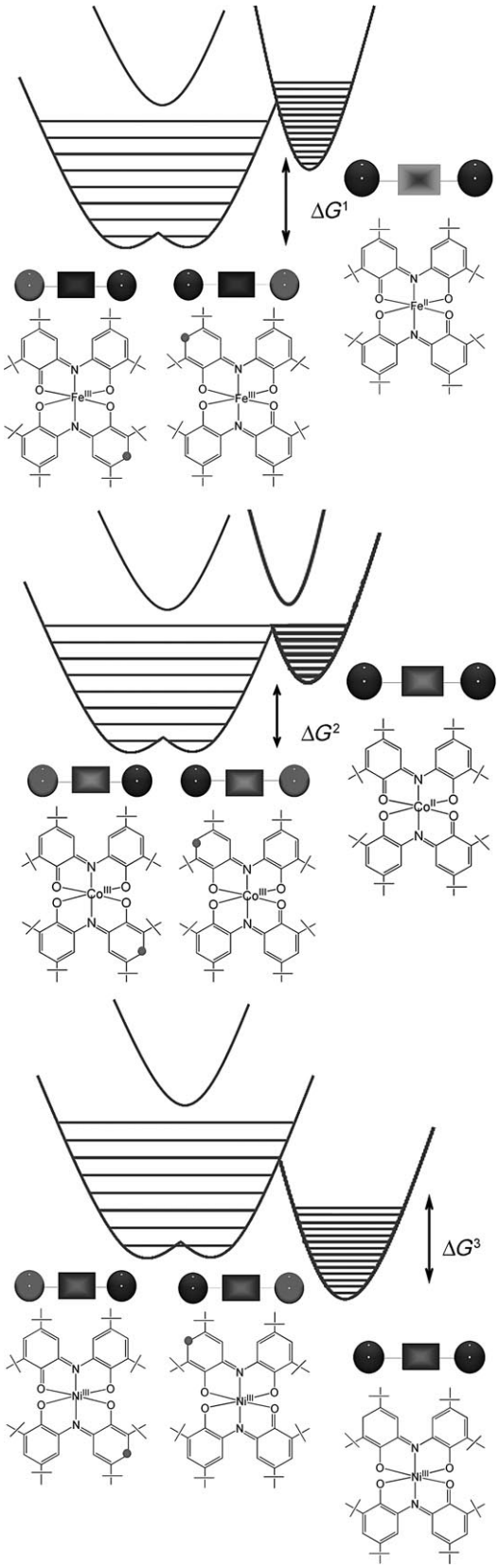

Figure 9. Resulting potential energy curve considering the two different electron transfer mechanisms present in complexes **2**–**4**.

ready reported. In fact, Tanaka et al.[28] have recently reported complexes with the general formula [Ni(L)-(tBu$_2$SQ)]·PF_6 as the first examples for the successful control of valence tautomerism between the Ni^{II}-SQ^{-} and Ni^{III}-Cat^{2-} frameworks, whereas Shimazaki et al.[29] have also recently reported that the one-electron oxidized form of a new mononuclear Ni^{II}-bis(salicylidene)diamine complex exhibits valence tautomerism. On the other hand, Banerjee et al[30] reported a semiquinone-catecholate based mixed valence complex [Fe(bispicen)(Cl_4Cat)(Cl_4SQ)]·DMF (bispicen = *N*,*N*-bis(2-pyridylmethyl)-1,2-ethanediamine), for which valence tautomerism has been followed by electronic absorption spectroscopy. The tautomer [Fe^{III}(Cl_4Cat)-(Cl_4SQ)] is favored at low temperatures, whereas at higher temperatures the [Fe^{II}(Cl_4SQ)$_2$] tautomer is the predominant form. This fact clearly reflects the importance of a good interplay between the metal ion and ligand-based orbitals.

Intermolecular electron transfer ligand-to-ligand (IET^{LL}): Another important question that has been raised within this family of complexes containing mixed-charge ligands Cat-N-BQ^{-} and Cat-N-SQ^{2-} is the possibility to exhibit intramolecular ligand-to-ligand (IET^{LL}) electron transfer phenomena. These complexes can be considered as inverted frameworks in which the redox-active moieties (i.e. iminoquinone ligands) are organic in nature and are electronically coupled through the metal-ion bridge that can promote the IET between them. Interestingly, our ^{1}H NMR experiments indicate that the extra electron, in such unusual family of mixed-valence complexes, can not be formally considered as localized within one of the ligands Cat-N-SQ^{2-}, but rather is delocalized over both of them. This result is supported by theoretical calculations. However, at this point, it is not possible to classify such IET either as a Class II or Class III system. Indeed, the equivalency between tBu groups found by ^{1}H NMR is not enough to assign it as a Class III system, as it is rather a slow probe ($\approx 10^{-9}$ s) on the electron transfer time scale. For this reason, additional evidence of other techniques that ensure faster probe data, such as vibrational spectroscopy, is highly required. Fortunately, resonance Raman (rR) studies of complexes **2** and **3** have already been reported in the literature.[31] The room-temperature (rR) spectrum of such complexes contains the vibrations of both electronic forms of the ligand, signifying that the ligands are not equivalent. Therefore, by comparing these results with those obtained for the slower probe ^{1}H NMR technique, we can assign IET^{LL} within this family of complexes as a Class II system.

Conclusion

The IET in the series of complexes [M(Cat-N-BQ)(Cat-N-SQ)], in which M = Co (**2**), Fe (**3**), and Ni (**4**) has been thoroughly revisited. Starting from a formal [M(Cat-N-BQ)(Cat-N-SQ)] picture, different scenarios involving IET^{LM} and IET^{LL} may lead to electron trapping on the metal ion or ligands. Complex **4**,*hs*-Ni^{II} does not exhibit any IET process, whereas complex **3**,*ls*-Fe^{III} only exhibits IET^{LM}, as a result of its mixed-valence character. Finally, our combined experimental and theoretical results indicate that complex **2** exhibits both IET^{LM} and IET^{LL}. The first process has been unequivocally associated to a reversible electron transfer between the metal ion and the ligand, although the latter corresponds to an intramolecular ligand-to-ligand electron-transfer phenomenon that takes place within the low-spin tautomer [M(Cat-N-BQ)(Cat-N-SQ)], with formally mixed-charge ligands. This is one of the few complexes so far reported to exhibit, simultaneously, two types of IET processes.

Although the origin of the intramolecular electron-transfer processes (IET^{LM} and IET^{LL}) is different, both can be formally considered as Class II systems according to the Robin and Day classification.[27] In the case of IET^{LL} the coupling between the (Cat-N-BQ)$^{-}$ and (Cat-N-SQ)$^{2-}$ ligands should be rather small, owing to the quasi-orthogonality of the π-type and metal-ion valence orbitals. Therefore, one may think that interligand electron hopping should proceed through other mechanisms, such as a solvent shell or tunnelling mechanism, as already indicated by Pierpont et al.[19c] This was the case for the [Ga(tmeda)(3,6-DBSQ)(3,6-DBCat)] (3,6-DBCat and 3,6-DBSQ refer to the catecholate and semiquinonate forms of 3,5-di-*tert*-butyl-*o*-quinone, respectively) complex in which no significant π bonding of the quinone ligands with the metal ion was observed. The use of more than one d orbital of the metal ion along the IET^{LL} process could also be invoked, although this process seems to be independent of the nature of the metal in the light of our theoretical inspection. This is not the case for IET^{LM}, which is strongly dependent on the nature of the metal ion. According to the different ionization potentials of the Co, Fe, and Ni metal ions, the overlap of the metal-centered orbitals with respect to the iminoquinone ligand π orbitals is modified, therefore, altering the electron transfer.

Experimental Section

All the reagents used were purchased from Aldrich and Fluka and used as received unless otherwise specified. Complexes **2**–**6** were synthesized as previously described.[20,21]

Physical measurements: Electronic absorption spectra were recorded by using a Varian Cary05e spectrophotometer equipped with a thermostated cell holder that can operate between 280 and 370 K. Temperature stability was better than ±5 K. Spectra were collected after the sample had been allowed to thermally equilibrate at each temperature for 10 min. T_c, the temperature at which the isomer ratio is 1:1, was deduced from the temperature at which the peaks of the low spin and the high spin exhibit similar intensities. The operating temperature window for each solvent does not enable us to collect the absorption of the pure low and high-spin species, and therefore, to have an accurate estimation of T_c. Direct current (dc) magnetic susceptibility measurements were carried out by using a Quantum Design MPMS SQUID susceptometer with a 55 kG magnet and operating in the range of 1.7–320 K. All measurements were collected in a field of 10 kG. Background correction data were collected from magnetic susceptibility measurements on the holder capsules. Diamagnetic corrections estimated from the Pascal contents were applied to

all data for determination of the molar paramagnetic susceptibilities of the compounds. NMR spectra were recorded by using a Bruker AV400 spectrometer equipped with a 5 mm triple resonance inverse probe with a dedicated ^{31}P channel operating at 500.33 MHz for ^{1}H equipped with a BVT3000 variable-temperature unit. TMS was used as an internal reference.

Evans method: This method is suitable for the calculation of the number of unpaired electrons in solution samples and is based on the frequency shift of the NMR signal of a reference sample by the magnetic field of a co-dissolved paramagnetic species. The relative frequency shift $\Delta\nu/\nu$ with $\Delta\nu = \nu$TMS(outer tube)$-\nu$TMS(inner tube), produced by the presence of the paramagnetic species is used to calculate the magnetic moment according to Equation (4):[32]

$$\chi_g = \chi_0 + [(3\Delta\nu)/(2\pi\nu_0 c)] + \{[(\chi_0(\rho_0 - \rho_s)]/c\} \quad (4)$$

in which χ_g = mass magnetic susceptibility of the solute ($cm^3 g^{-1}$); χ_0 = magnetic susceptibility of the solvent ($cm^3 g^{-1}$); $\Delta\nu$ = separation in paramagnetic chemical shift (Hz); ν_0 = spectrometer radiofrequency; c = concentration ($mol\,mL^{-1}$); ρ_0 = density of the pure solvent and ρ_s = density of the solution. Equation (4) can be transformed then to Equation (5):

$$\chi_m = \chi_0 M' + [(3\Delta\delta \times 10^{-6})/(4\pi c)] \quad (5)$$

From Equation (5) you obtain Equation (6) by taking into account the diamagnetic contribution, which can be estimated as the sum of constants (called Pascal's constants) for each diamagnetic species in the sample [Eq. (7)]:

$$\chi_m^{corr} = \chi_m - \Sigma\chi_\alpha \quad (6)$$

$$\chi_m^{corr} = \chi_0 M' + [(3\Delta\delta \times 10^{-6})/(4\pi c)] - \Sigma\chi_\alpha \quad (7)$$

Finally, the χ_m^{corr} obtained from Equation (7) is used to calculate the effective magnetic moment as shown in Equation (8):

$$\mu_{eff} = 2.828\sqrt{(\chi_m^{corr} T)} \quad (8)$$

The NMR samples for susceptibility measurements using the Evans Method were prepared by dissolving a weighted amount of complex **1**, **2**, and **3** in a measured volume of solvent. All the experiments are done in deuterated solvents. The concentration of the paramagnetic solute was in the range of 1–3 $mg\,mL^{-1}$. The temperature-dependent density changes of the solvent were corrected by using equations and data from the International Critical Tables.[33] The complex solution was transferred into a 5 mm tube containing a 1 mm capillary with the deuterated diamagnetic solvent and one drop of tetramethylsilane (TMS) as a reference. The different signal shifts found for the methyl groups of the TMS was used to determine the susceptibility in solution.

Computational details: Both density functional theory (DFT)-based and wavefunction-based ab initio quantum chemical approaches have reached a level of accuracy, which allows one to give some relevant insights into the electronic phenomena. It is known that explicitly correlated calculations are powerful tools to extract both information upon excitation energies and microscopic representations of the ground and excited states. On the other hand, DFT calculations are very reliable in the determination of equilibrium geometries, understanding of IR and UV spectra, but may suffer from their intrinsic single-reference character. Methods that use the exact Hamiltonian do not suffer from the arbitrariness of the mutiparametrization of the exchange correlation potential in DFT-based techniques. For those reasons, wavefunction calculations are particularly appealing. since the multireference character of the description gives access to important information with respect to the weights of the different relevant configurations.[34] The efficiency of ab initio techniques has been demonstrated in the study of magnetically coupled molecular were conducted. More recently, spectroscopic accuracy has also been reached and intriguing electronic distributions have been unravelled for the important class of non-innocent ligand-based metal complexes.[35] In the context of this study, wavefunction calculations were preferred since our goal is to look for the microscopic origin of competing spin states which may be attributed to electron transfer phenomena. Not only how effective is the intramolecular electron transfer but also to what extent both Cat-N-BQ^- ligands are involved in the process remain challenging questions. The one-electron basis sets employed to describe the molecular orbitals (MOs) are derived from primitive atomic natural orbitals (ANOs) (17s12p9d4f) for iron, nickel, and cobalt, respectively. These basis sets were contracted into [7s6p4d1f]. Regarding the lighter elements C and N, we used (10s6p3d)/[3s2p1d], and O (10s6p3d)/[3s3p1d] contractions. Finally, hydrogen atoms were described with minimal basis set (3s)/[1s]. The zero-order wavefunction is formed by a linear expansion of Slater determinants. Such description is accessible by means of complete active space self-consistent field (CASSCF) calculations which incorporate qualitatively the leading electronic configurations distributing n electrons in m MOs, defining an active space referenced as CAS(n,m). At this level of calculation, the so-called static correlation effects are taken into account, provided that the active space is flexible enough. Depending on the number of d electrons for the various systems at hands, the CAS which can be anticipated consists of the mainly d-type orbitals and a mainly ligand type orbitals possibly singly-occupied. However, such procedure fails to reproduce the correct relative energies since dynamical correlation effects are not incorporated. These predominantly atomic effects can be incorporated within different framework on top of the CASSCF wavefunction. In this respect, complete active space second-order perturbation theory (CASPT2) calculations have proven to be impressive tools to accurately investigate spectroscopy issues. All CASPT2 calculations were performed with an imaginary shift of 0.2 Hartree to avoid the presence of intruder states. All electrons were correlated except those in the core parts. Both CASSCF and CASPT2 procedures are available in the Molcas 6.0 package we used throughout the theoretical analysis.[36]

Acknowledgements

This work was supported by the Spanish Government under MAT 2009-13977-C03-03 and the Network of Excellence MAGMAnet.This work was also supported by the Comunitat de Treball dels Pirineus/Communauté de Travail des Pyrénées program for cooperation, research, and technological development.

[1] a) P. Gütlich, Y. Garcia, T. Woike, *Coord. Chem. Rev.* **2001**, *219*, 839–879; b) O. Kahn, J. P. Launay, *Chemtronics* **1988**, *3*, 140–151; c) A. Hauser, *Coord. Chem. Rev.* **1991**, *111*, 275–290.
[2] N. Sutin, *Acc. Chem. Res.* **1982**, *15*, 275–282.
[3] C. Creutz, H. Taube, *J. Am. Chem. Soc.* **1969**, *91*, 3988–3989.
[4] a) M. D. Ward, *Chem. Ind.* **1996**, 568–573; b) R. Ziessel, M. Hissler, A. El-Ghayoury, A. Harriman, *Coord. Chem. Rev.*. **1998**, *178–180*, 1251–1298; c) M. N. Paddon-Row, *Acc. Chem. Res.* **1994**, *27*, 18–25; d) M. R. Wasielewski, *Chem. Rev.* **1992**, *92*, 435–461; e) J. P. Launay, *Chem. Soc. Rev.* **2001**, *30*, 386–397.
[5] a) T. M. Figueira-Duarte, V. Lloveras, J. Vidal-Gancedo, A. Gégout, B. Delavaux-Nicot, R. Welter, J. Veciana, C. Rovira, J.-F. Nierengarten, *Chem. Commun.* **2007**, 4345–4347; b) S. Barlow, D. O'Hare, *Chem. Rev.* **1997**, *97*, 637–670, and references therein.
[6] For a general review on pure organic mixed-valence systems, see: D. Ruiz-Molina, J. Sedó, C. Rovira, J. Veciana in *Handbook of Advanced Electronic Materials and Devices* (Ed.: H. S. Nalwa), Hardbound, Academic Press, **2001**, pp. 303–327, and references therein.
[7] a) S. F. Rak, L. L. J. Miller, *J. Am. Chem. Soc.* **1992**, *114*, 1388–1394; b) L. L. Miller, C. A. Liberko, *Chem. Mater.* **1990**, *2*, 339–340, and references therein.
[8] a) I. Danila, F. Biaso, H. Sidorenkova, M. Geoffroy, M. Fourmigue, E. Levillain, N. Avarvari, *Organometallics* **2009**, *28*, 3691–3699; b) M. Iyoda, M. Hasegawa, Y. Miyake, *Chem. Rev.* **2004**, *104*, 5085–

5113; c) T. Otsubo, Y. Aso, K. Takimiya, *Adv. Mater.* **1996**, *8*, 203–211; d) J. Y. Becker, J. Bernstein, A. Ellern, H. Gershtenman, V. J. Khodorkovsky, *Mater. Chem.* **1995**, *5*, 1557–1558; e) K. Lahlil, A. Moradpour, C. Bowlas, F. Menou, P. Cassoux, J. Bonvoisin, J. P. Launay, G. Dive, D. Dehareng, *J. Am. Chem. Soc.* **1995**, *117*, 9995–10002.

[9] a) R. Sakamoto, T. Sasaki, N. Honda, T. Yamamura, *Chem. Commun.* **2009**, 5156–5158; b) S. F. Nelsen, H. Q. Tran, M. A. Nagy, *J. Am. Chem. Soc.* **1998**, *120*, 298–304; c) S. F. Nelsen, R. F. Ismagilov, Y. Teki, *J. Am. Chem. Soc.* **1998**, *120*, 2200–2201.

[10] A. Dei, D. Gatteschi, C. Sangregorio, L. Sorace, *Acc. Chem. Res.* **2004**, *37*, 827.

[11] a) J. Bonvoisin, J. P. Launay, M. Van der Auweraer, F. C. De Schryver, *J. Phys. Chem.* **1994**, *98*, 5052–5057; b) C. Lambert, G. Nöll, *J. Am. Chem. Soc.* **1999**, *121*, 8434–8442; c) S. Utamapanya, A. Rajca, *J. Am. Chem. Soc.* **1991**, *113*, 9242–9251; d) O. Elsner, D. Ruiz-Molina, J. Vidal-Gancedo, C. Rovira, J. Veciana, *Nano Lett.* **2001**, *1*, 117–120; e) J. Sedó, D. Ruiz, J. Vidal-Gancedo, C. Rovira, J. Bonvoisin, J. P. Launay, J. Veciana, *Adv. Mater.* **1996**, *8*, 748–752.

[12] a) S. F. Nelsen, M. N. Weaver, J. P. Telo, *J. Am. Chem. Soc.* **2007**, *129*, 7036–7043; b) C. Risko, S. Barlow, V. Coropceanu, M. Halik, J. L. Bredas, S. R. Marder, *Chem. Commun.* **2003**, 194–195.

[13] a) B. P. Sullivan, H. Abruña, H. O. Finklea, D. J. Salmon, J. K. Nagle, T. J. Meyer, H. Sprintsxhnik, *Chem. Phys. Lett.* **1978**, *58*, 389–393; b) C. F. Shu, M. S. Wrighton, *Inorg. Chem.* **1988**, *27*, 4326–4329; c) A. B. P. Lever, *Inorg. Chem.* **1990**, *29*, 1271–1285; d) A. B. P. Lever, *Inorg. Chem.* **1991**, *30*, 1980–1985.

[14] a) A. A. Vleček, *Coord. Chem. Rev.* **1982**, *43*, 39–62; b) B. K. Ghosh, A. Chakravorty, *Coord. Chem. Rev.* **1989**, *95*, 239–294; c) A. Juris, V. Balzani, S. Campagna, F. Barigelletti, P. Belser, A. V. Zelewesky, *Coord. Chem. Rev.* **1988**, *84*, 85–277; d) C. G. Pierpont, C. W. Lange, *Prog. Inorg. Chem.* **1993**, *0-0*, 331–342.

[15] Y. Sasaki, M. Abe, *Chem. Rec.* **2004**, *4*, 279–290, and references therein.

[16] E. Evangelio, D. N. Hendrickson, D. Ruiz-Molina, *Inorg. Chim. Acta* **2008**, *361*, 3403–3409.

[17] a) E. Evangelio, D. Ruiz-Molina, *Eur. J. Inorg. Chem.* **2005**, 2957–2971; b) E. Evangelio, D. Ruiz-Molina, *C. R. Chim.* **2008**, *11*, 1137–1154; c) D. N. Hendrickson, C. G. Pierpont, *Top. Curr. Chem.* **2004**, *34*, 63–95; d) P. Gütlich, A. Dei, *Angew. Chem.* **1997**, *109*, 2852–2855; *Angew. Chem. Int. Ed. Engl.* **1997**, *36*, 2734–2736; e) C. G. Pierpont, S. Kitagawa, *Inorganic Chromotropism*, Kodansha/Springer, Tokyo, **2007**, pp. 116–142; f) C. G. Pierpont, R. M. Buchanan, *Coord. Chem. Rev.* **1981**, *38*, 45–87; g) O. Sato, J. Tao, Y.-Z. Zhang, *Angew. Chem.* **2007**, *119*, 2200–2236; *Angew. Chem. Int. Ed.* **2007**, *46*, 2152–2187; h) D. A. Schultz in *Magnetism: Molecules to Materials, Vol. II* (Eds.: J. S. Miller, M. Drillon), Wiley-VCH, Weinheim, **2001**, p. 81.

[18] a) D. Kiriya, H.-C. Chang, S. Kitagawa, *J. Am. Chem. Soc.* **2008**, *130 (16)*, 5515–5522; b) D. Kiriya, H.-C. Chang, A. Kamata, S. Kitagawa, *Dalton Trans.* **2006**, 1377–1382; c) M. Adams, A. Dei, A. L. Rheingold, D. N. Hendrickson, *Angew. Chem.* **1993**, *105*, 954–956; *Angew. Chem. Int. Ed. Engl.* **1993**, *32*, 880–882; d) D. M. Adams, A. Dei, A. L. Rheingold, D. N. Hendrickson, *J. Am. Chem. Soc.* **1993**, *115*, 8221–8229; e) O. S. Jung, D. H. Jo, Y. A. Lee, B. J. Conklin, C. G. Pierpont, *Inorg. Chem.* **1997**, *36*, 19–24; f) O. S. Jung, C. G. Pierpont, *J. Am. Chem. Soc.* **1994**, *116*, 2229–2230; g) O. S. Jung, D. H. Lee, Y. S. Sohn, C. G. Pierpont, *Inorg. Chem.* **1998**, *37*, 5875–5880; h) S. Bin-Salamon, S. H. Brewer, E. C. Depperman, S. Franzen, J. W. Kampf, M. L. Kirk, R. K. Kumar, S. Lappi, K. Peariso, K. E. Preuss, D. A. Schultz, *Inorg. Chem.* **2006**, *45*, 4461–4467; i) A. Beni, A. Dei, D. A. Schultz, L. Sorace, *Chem. Phys. Lett.* **2006**, *428*, 400–404.

[19] The coexistence of two IET within this family of complexes was already pointed out some time ago: a) S. P. Solodovnikov, N. N. Bubnov, A. I. Prokof'ev, *Usp. Khim.* **1980**, *49*, 1; b) R. R. Rakhimov, S. P. Solodovnikov, V. S. Pupkov, A. I. Prokof'ev, *Izv. Akad. Nauk SSSR* **1990**, 1385; c) C. W. Lange, B. J. Conklin, C. G. Pierpont, *Inorg. Chem.* **1994**, *33*, 1276–1283; d) D. M. Adams, L. Noodleman, D. N. Hendrickson, *Inorg. Chem.* **1997**, *36*, 3966–3984.

[20] a) S. K. Larsen, C. G. Pierpont, *J. Am. Chem. Soc.* **1988**, *110*, 1827–1832; b) A. Caneschi, A. Cornia, A. Dei, *Inorg. Chem.* **1998**, *37*, 3419–3421.

[21] C. L. Simpson, S. R. Boone, C. G. Pierpont, *Inorg. Chem.* **1989**, *28*, 4379–4385.

[22] a) O. Hayaishi, M. Nozaki, *Science* **1969**, *164*, 389.396; b) C. A. Tyson, A. E. Martell, *J. Am. Chem. Soc.* **1972**, *94*, 939–945; c) A. Y. Girgis, A. L. Balch, *Inorg. Chem.* **1975**, *14*, 2724–2727; d) L. A. DeLaire, R. C. Haltiwanger, C. G. Pierpont, *Inorg. Chem.* **1989**, *28*, 644–650.

[23] This ligand may sometimes exhibit a more complicated behavior: P. Chaudhuri, M. Hess, K. Hildebrand, E. Bill, T. Weyhermüller, K. Wieghardt, *Inorg. Chem.* **1999**, *38*, 2781–2790.

[24] a) O. Cador, F. Chabre, A. Dei, C. Sangregorio, J. V. Slageren, M. G. F. Vaz, *Inorg. Chem.* **2003**, *42*, 6432–6440; b) P. L. Gentili, L. Bussotti, R. Righini, A. Beni, L. Bogani, A. Dei, *Chem. Phys.* **2005**, *314*, 9–17.

[25] D. F. Evans, *J. Chem. Soc.* **1959**, 2003–2005.

[26] N. S. Hush, *Prog. Inorg. Chem.* **1967**, *8*, 391–444.

[27] M. B. Robin, P. Day, *Adv. Inorg. Chem. Radiochem.* **1968**, *10*, 247–422.

[28] H. Ohtsu, K. Tanaka, *Angew. Chem.* **2004**, *116*, 6461–6463; *Angew. Chem. Int. Ed.* **2004**, *43*, 6301–6303.

[29] Y. Shimazaki, F. Tani, K. Fukui, Y. Naruta, O. Yamauchi, *J. Am. Chem. Soc.* **2003**, *125*, 10512–10513.

[30] N. Shaikh, S. Goswami, A. Panja, X.-Y. Wang, S. Gao, R. J. Butcher, P. Banarjee, *Inorg. Chem.* **2004**, *43*, 5908–5918.

[31] S. Bruni, A. Caneschi, F. Cariati, C. Delfs, A. Dei, D. Gatteschi, *J. Am. Chem. Soc.* **1994**, *116*, 1388–1394.

[32] S. K. Sur, *J. Magn. Reson.* **1989**, *82*, 169–173.

[33] Values obtained from: I. Cibulka, T. Takagi, *J. Chem. Eng. Data* **1999**, *44*, 411.

[34] A. Sadoc, C. de Graaf, R. Broer, R. *Phys. Rev. B,* **2007**, *75*, 165116–165124.

[35] a) D. Herebian, K. Wieghardt, F. Neese, *J. Am. Chem. Soc.* **2003**, *125*, 10997–11005; b) S. Messaoudi, V. Robert, N. Guihéry, D. Maynau, *Inorg. Chem.* **2006**, *45*, 3212–3216; c) D. J. Brook, V. Lynch, B. Conklin, M. A. Fox, *J. Am. Chem. Soc.* **1997**, *119*, 5155–5162.

[36] a) G. Karlström, R. Lindh, P.-A. Malmqvist, B. O. Roos, U. Ryde, V. Veryazov, P.-O. Widmark, M. Cossi, B. Schimmelpfennig, P. Neogrady, L. Seijo, *Computational Materials Science* **2003**, *28*, 222–239.

Received: September 17, 2009
Published online: April 23, 2010

